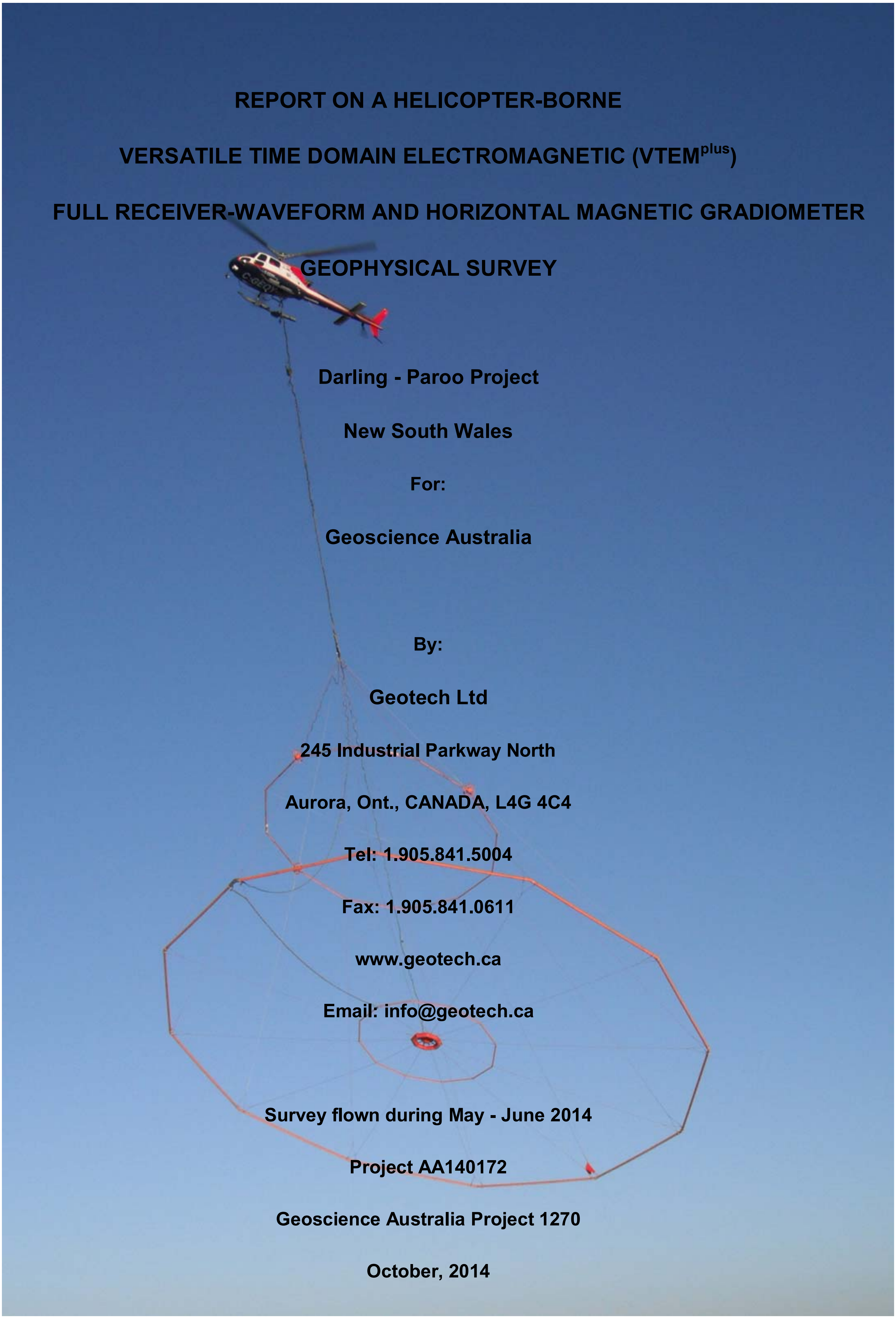

REPORT ON A HELICOPTER-BORNE

VERSATILE TIME DOMAIN ELECTROMAGNETIC (VTEM^{plus})

FULL RECEIVER-WAVEFORM AND HORIZONTAL MAGNETIC GRADIOMETER

GEOPHYSICAL SURVEY

Darling - Paroo Project

New South Wales

For:

Geoscience Australia

By:

Geotech Ltd

245 Industrial Parkway North

Aurora, Ont., CANADA, L4G 4C4

Tel: 1.905.841.5004

Fax: 1.905.841.0611

www.geotech.ca

Email: info@geotech.ca

Survey flown during May - June 2014

Project AA140172

Geoscience Australia Project 1270

October, 2014

TABLE OF CONTENTS

LIST OF FIGURES

LIST OF TABLES

APPENDICES

REPORT ON A HELICOPTER-BORNE VERSATILE TIME DOMAIN ELECTROMAGNETIC (VTEM^{plus}) FULL RECEIVER-WAVEFORM and HORIZONTAL MAGNETIC GRADIOMETER GEOPHYSICAL SURVEY

Darling Paroo Project
New South Wales

EXECUTIVE SUMMARY

From May 11th to June 4th 2014 Geotech Ltd. carried out a helicopter-borne geophysical survey over Darling Paroo Project in New South Wales. Operations base were re-located three times during the survey, Bourke, New South Wales (May 9th to May 12th 2014), Tilpa, New South Wales (May 13th to May 23rd 2014) and Menindee, New South Wales (May 24th to June 4th 2014).

Principal geophysical sensors included a versatile time domain electromagnetic (VTEM^{plus}) full receiver-waveform system, and horizontal magnetic gradiometer. Ancillary equipment included a GPS navigation system, laser and radar altimeters, and inclinometer. A total of 2657 line-kilometres of geophysical data were acquired during the survey.

In-field data quality assurance and preliminary processing were carried out on a daily basis during the acquisition phase. Preliminary and final data processing, including generation of final digital data products were undertaken from the office of Geotech Ltd. in Aurora, Ontario.

Digital data includes all electromagnetic and magnetic data, conductivity imaging products, mulitplots plus ancillary data including the waveform.

This survey report describes the procedures for data acquisition, processing, final image presentation and the specifications for the digital data set.

1. INTRODUCTION

1.1 General Considerations

Geotech Ltd performed a helicopter-borne geophysical survey over Darling Paroo Project in New South Wales (Figure 1 & Figure 2).

Mr. Murray Richardson and Dr. Ross Brodie represented Geoscience Australia during the data acquisition and data processing phases of this project respectively.

The geophysical survey consisted of helicopter borne EM using the versatile time-domain electromagnetic (VTEM^{plus}) full receiver-waveform streamed data recording system with Z and X component measurements and horizontal magnetic gradiometer using two cesium magnetometers. A total of 2657 line-km of geophysical data were acquired during the survey.

The crew was based out of Bourke, Tilpa and Menindee (Figure 2) in New South Wales for the acquisition phase of the survey. Survey flying started on May 11th 2014 and was completed on June 4th, 2014.

Data quality control and quality assurance, and preliminary data processing were carried out on a daily basis during the acquisition phase of the project. Final data processing followed immediately after the end of the survey. Final reporting, data presentation and archiving were completed from the Aurora office of Geotech Ltd in October, 2014.

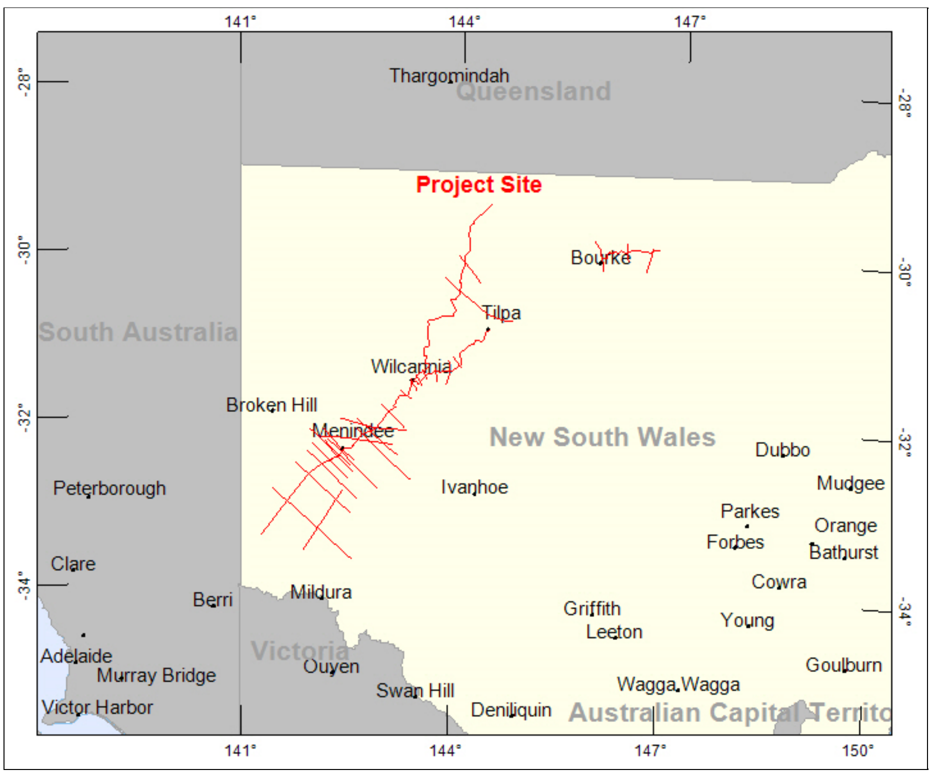

Figure 1: Survey Location.

1.2 Survey Location

The survey areas are located near Bourke, Tilpa and Menindee in New South Wales (Figure 2).

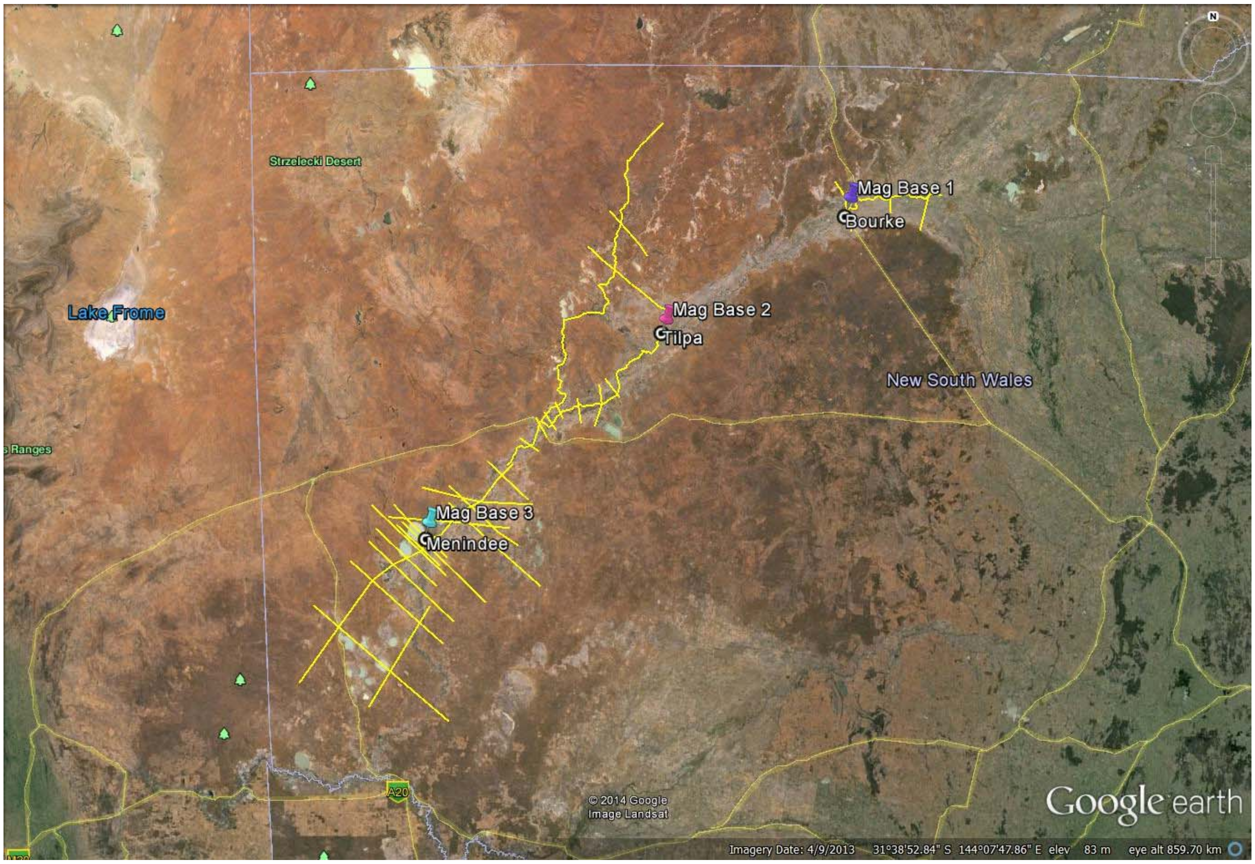

Figure 2: Survey area location on Google Earth.

The survey consisted of two parts:

1. Darling Paroo survey lines using a waveform with an on-time pulse of 7.33 ms (Figure 4)
2. Selected lines from part 1 were flown using a different waveform with a shorter on-time pulse of 4.74 ms (Figure 5).

1.3 Topographic Relief and Cultural Features

Topographically, the survey area exhibits a nearly level relief with an elevation ranging from 35 to 128 metres above mean sea level over an area of 252,752 square kilometres (Figure 3).

There are various ephemeral rivers and streams running through the survey area which connect various lakes. There are visible signs of culture such as roads, mine location, power lines, railways and pipelines located in the survey area.

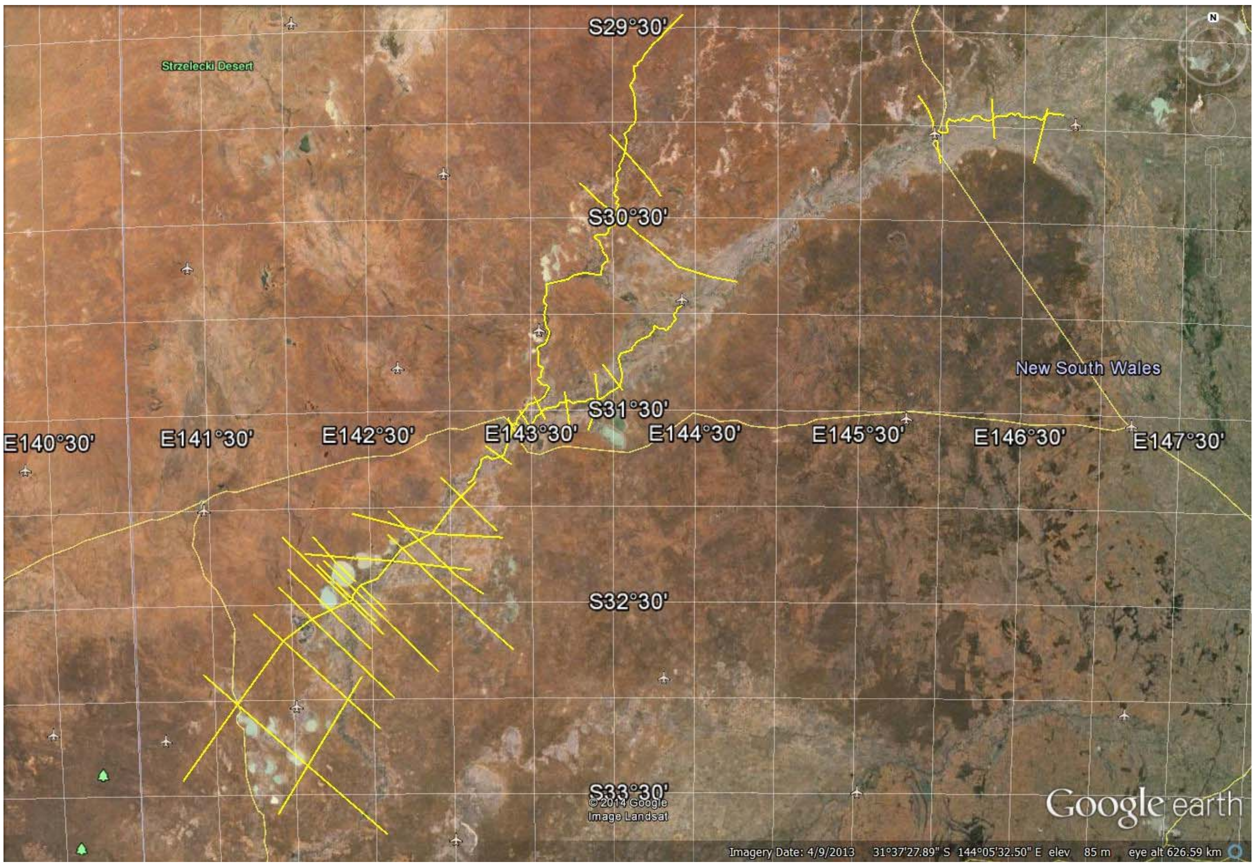

Figure 3: Flight path over a Google Earth image

2. DATA ACQUISITION

2.1 Flight Line Specifications

The regional survey block (see Figure 3 and Appendix A) and general flight line specifications are as follows:

Table 1: Survey Specifications

Survey block	Line spacing (m)	Area (km^2)	Planned[1] Line-km	Actual Line-km	Flight direction	Line numbers
Darling Paroo	n/a	252,752	2393	2498	Variable	L100 – L3201
Short Pulse	n/a	n/a	155	159	Variable	L505 – L605
TOTAL		**252,752**	**2548**	**2657**		

Survey area boundary co-ordinates in WGS84 Zone 54 South coordinate system are as follows:

X	Y
514398.2	6258353.7
514398.2	6786663.6
1069588.9	6786663.6
1069588.9	6258353.7

2.2 Flying Height Specifications

During the survey the helicopter was maintained at a mean altitude of 73 metres above the ground with an average survey speed of 87 km/hour. This allowed for an actual average EM Transmitter-receiver loop terrain clearance of 43 metres and a magnetic sensor clearance of 50 metres.

2.3 Survey Operations

Survey operations were based out of Bourke, Tilpa and Menindee in New South Wales from May 9th, 2014 to June 4th 2014. The following table shows the timing of the flying.

Table 2: Survey schedule

Date	Flight #	Flown km	Block	Crew location	Comments
9-May-2014				Bourke, NSW	Test flight
10-May-2014				Bourke, NSW	Test flight
11-May-2014	1.2	179		Bourke, NSW	179km flown
12-May-2014				Bourke, NSW	Relocate to new base (Tilpa)
13-May-2014	3,4,5	458		Tilpa, NSW	458km flown

[1] Note: Actual line kilometres represent the total line kilometres in the final database. These line kilometres normally exceed the planned line kilometres, as indicated in the survey NAV files.

Date	Flight #	Flown km	Block	Crew location	Comments
14-May-2014				Tilpa, NSW	Crew change
15-May-2014	6,7,8	369		Tilpa, NSW	369km flown
16-May-2014				Tilpa, NSW	No production Vehicle repairs
17-May-2014				Tilpa, NSW	No production Vehicle repairs
18-May-2014				Tilpa, NSW	No production Vehicle repairs
19-May-2014				Tilpa, NSW	No production Vehicle repairs
20-May-2014				Tilpa, NSW	No production Vehicle repairs
21-May-2014				Tilpa, NSW	No production Vehicle repairs
22-May-2014				Tilpa, NSW	No production Vehicle repairs
23-May-2014				Tilpa, NSW	Relocated to Menindee
24-May-2014	9,10,11	248		Menindee, NSW	248km flown
25-May-2014	12,13,14	416		Menindee, NSW	416km flown
26-May-2014				Menindee, NSW	No production due to weather
27-May-2014				Menindee, NSW	No production due to weather
28-May-2014	15,16	306		Menindee, NSW	306km flown
29-May-2014	17,18,19	372		Menindee, NSW	372km flown
30-May-2014	20,21	192		Menindee, NSW	192km flown
31-May-2014				Menindee, NSW	No production due to weather
1-June-2014				Menindee, NSW	No production due to weather
2-June-2014				Menindee, NSW	No production due to weather
3-June-2014				Menindee, NSW	Test flight
4-June-2014	22,23	155		Menindee, NSW	Remaining 155 kms were flown – flying complete

2.4 Procedures

The on board operator was responsible for monitoring the system integrity. He also maintained a detailed flight log during the survey, tracking the times of the flight as well as any unusual geophysical or topographic features.

On return of the aircrew to the base camp the survey data was transferred from a compact flash card (PCMCIA) to the data processing computer. The data were then uploaded via ftp to the Geotech office in Aurora for daily quality assurance and quality control by qualified personnel.

2.5 Aircraft and Equipment

2.5.1 Survey Aircraft

The survey was flown using a Eurocopter Aerospatiale (Astar) 350 B3 helicopter, registration VH-VTN. The helicopter is owned and operated by United Aero Helicopters. Installation of the geophysical and ancillary equipment was carried out by a Geotech Ltd crew.

2.5.2 Electromagnetic System

The electromagnetic system was a Geotech Time Domain EM (VTEM^{plus}) with full receiver-waveform streamed data recording at 192 kHz. The "full waveform VTEM system" uses the streamed half-cycle recording of transmitter current and receiver voltage waveforms to obtain a complete system response calibration throughout the entire survey flight. VTEM hardware with the Serial number 12 was used for the survey. Two VTEM transmitter current waveforms were used for the survey with Figure 4 representing the waveform used for the main Darling Paroo lines and Figure 5 representing the waveform used for the Short Pulse survey lines.

The VTEM transmitter loop and Z-component receiver coils were in a concentric-coplanar configuration and their axes are nominally vertical. An X-component receiver coil was also installed in the centre of the transmitter loop, with its axis nominally horizontal and in the flight line direction. The receiver coils measure the dB/dt response, and a B-Field response is calculated during the data processing. The EM transmitter-receiver loop assembly was towed at a mean distance of 34 metres below the aircraft. The configuration is shown in Figure 6.

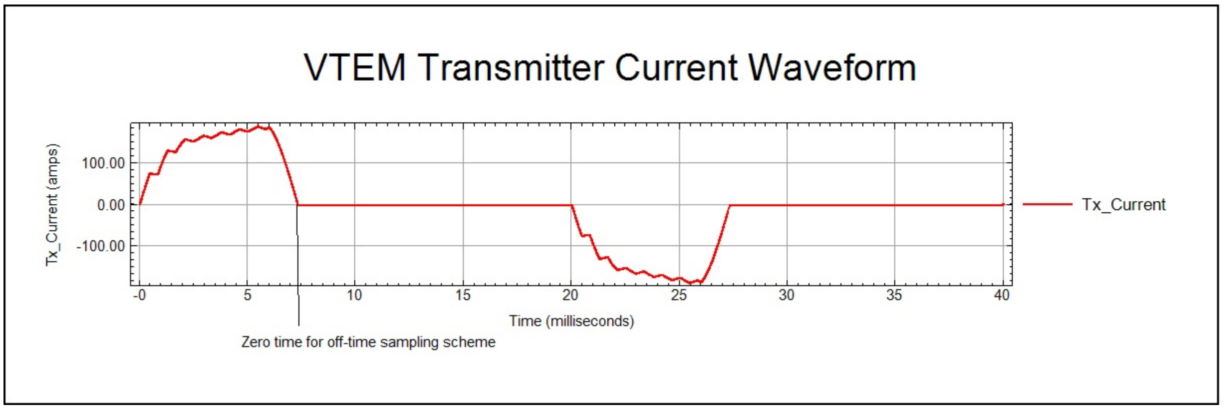

Figure 4: VTEM Transmitter Current Waveform for Darling Paroo Survey Lines

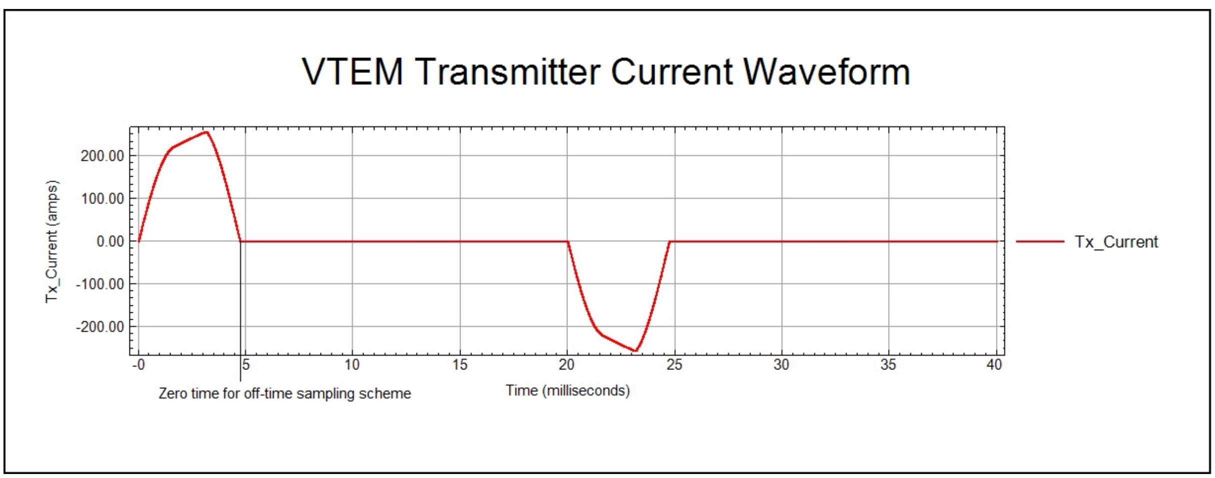

Figure 5: VTEM Transmitter Current Waveform for Short Pulse Survey Lines

The VTEM decay sampling scheme is shown in Table 3 below.

Forty-five time measurement gates were used for the final data processing of Darling Paroo survey lines data with gate centers in the range from 0.021 to 10.667 msec. Forty-six time measurement gates were used for the final data processing of short pulse data with gate centers in the range from 0.021 to 12.250 msec.

Zero time for the off-time sampling scheme is equal to the current pulse width and is defined as the time near the end of the turn-off ramp where the dI/dt waveform falls to 1/2 of its peak value.

Table 3: Off-Time Decay Sampling Scheme

VTEM Decay Sampling Scheme				
index	**Start**	**End**	**Middle**	**Width**
Milliseconds				
4	0.018	0.023	0.021	0.005
5	0.023	0.029	0.026	0.005
6	0.029	0.034	0.031	0.005
7	0.034	0.039	0.036	0.005
8	0.039	0.045	0.042	0.006
9	0.045	0.051	0.048	0.007
10	0.051	0.059	0.055	0.008
11	0.059	0.068	0.063	0.009
12	0.068	0.078	0.073	0.010
13	0.078	0.090	0.083	0.012
14	0.090	0.103	0.096	0.013
15	0.103	0.118	0.110	0.015
16	0.118	0.136	0.126	0.018
17	0.136	0.156	0.145	0.020
18	0.156	0.179	0.167	0.023
19	0.179	0.206	0.192	0.027
20	0.206	0.236	0.220	0.030
21	0.236	0.271	0.253	0.035
22	0.271	0.312	0.290	0.040
23	0.312	0.358	0.333	0.046
24	0.358	0.411	0.383	0.053
25	0.411	0.472	0.440	0.061
26	0.472	0.543	0.505	0.070
27	0.543	0.623	0.580	0.081
28	0.623	0.716	0.667	0.093
29	0.716	0.823	0.766	0.107
30	0.823	0.945	0.880	0.122
31	0.945	1.086	1.010	0.141
32	1.086	1.247	1.161	0.161
33	1.247	1.432	1.333	0.185

VTEM Decay Sampling Scheme				
index	Start	End	Middle	Width
Milliseconds				
34	1.432	1.646	1.531	0.214
35	1.646	1.891	1.760	0.245
36	1.891	2.172	2.021	0.281
37	2.172	2.495	2.323	0.323
38	2.495	2.865	2.667	0.370
39	2.865	3.292	3.063	0.427
40	3.292	3.781	3.521	0.490
41	3.781	4.341	4.042	0.560
42	4.341	4.987	4.641	0.646
43	4.987	5.729	5.333	0.742
44	5.729	6.581	6.125	0.852
45	6.581	7.560	7.036	0.979
46	7.560	8.685	8.083	1.125
47	8.685	9.977	9.286	1.292
48	9.977	11.458	10.667	1.482
49	11.458	13.161	12.250	1.703

Z Component: 4 - 48 time gates
X Component: 20 - 48 time gates.

Z Component for Short Pulse: 4 - 49 time gates
X Component for Short Pulse: 20 - 49 time gates.

VTEM system specifications:

Transmitter

Regular pulse

- Transmitter loop diameter: 26 m
- Number of turns: 4
- Transmitter loop area: 530.92 m^2
- Effective Transmitter loop area: 2123.7 m^2
- Transmitter base frequency: 25 Hz
- Peak current: 191 A
- Pulse width: 7.33 ms
- Wave form shape: Bi-polar trapezoid
- Peak dipole moment: 405,627 nIA
- Actual average EM transmitter-receiver loop terrain clearance: 43 metres above the ground

Short pulse

- Transmitter loop diameter: 26 m
- Number of turns: 4
- Transmitter loop area: 530.92 m^2
- Effective Transmitter loop area: 2123.7 m^2
- Transmitter base frequency: 25 Hz
- Peak current: 257 A
- Pulse width: 4.74 ms
- Wave form shape: Bi-polar trapezoid
- Peak dipole moment: 545,791 nIA
- Actual average EM transmitter-receiver loop terrain clearance: 43 metres above the ground

Receiver

- X Coil diameter: 0.32 m
- Number of turns: 245
- Effective coil area: 19.69 m^2
- Z-Coil diameter: 1.2 m
- Number of turns: 100
- Effective coil area: 113.04 m^2

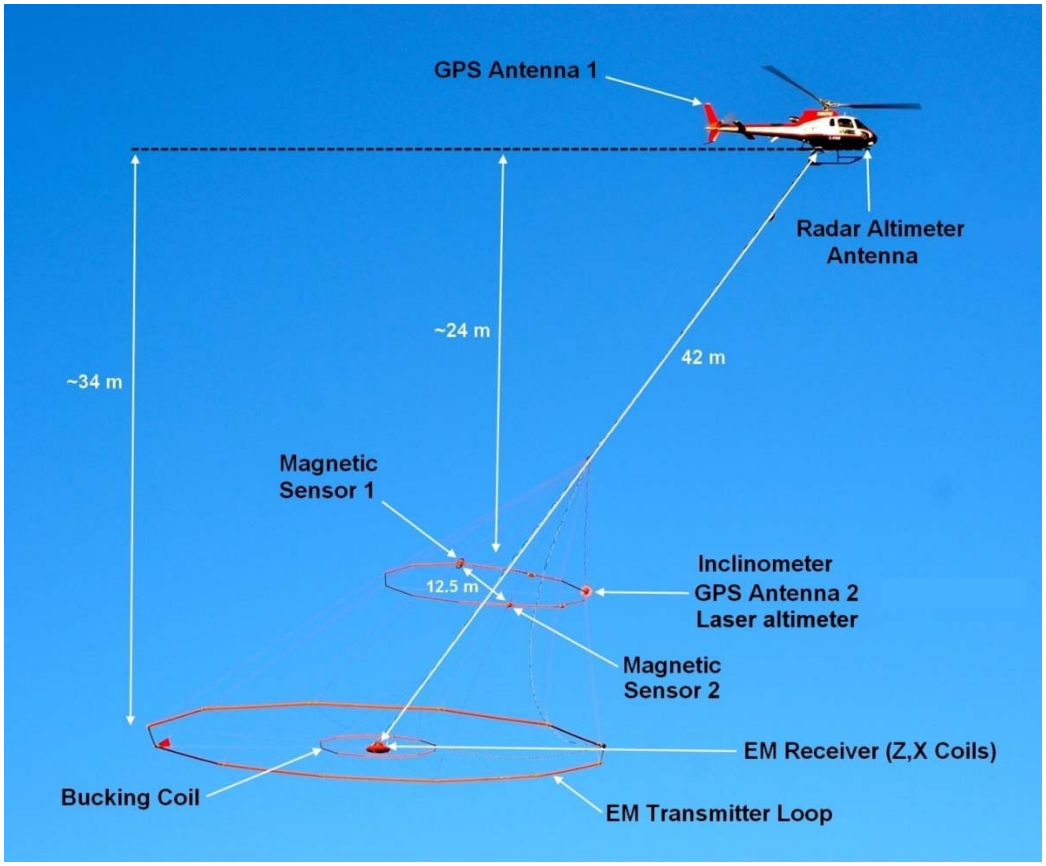

Figure 6: VTEM^{plus} System Configuration.

2.5.3 Horizontal Magnetic Gradiometer

The horizontal magnetic gradiometer consists of two Geometrics split-beam field magnetic sensors with a sampling interval of 0.1 seconds. These sensors are mounted 12.5 metres apart on the magnetic gradiometer loop 10 metres above the EM transmitter-receiver loop.

2.5.4 GPS Navigation System – Helicopter

The navigation system used a Geotech PC104 based navigation system utilizing NovAtel's WAAS (Wide Area Augmentation System) enabled GPS receiver, Geotech navigate software, a full screen display with controls in front of the pilot to direct the flight and a NovAtel GPS antenna mounted on the helicopter tail (Figure 6). As many as 11 GPS and two WAAS satellites may be monitored at any one time. The positional accuracy or circular error probability (CEP) is 1.8 m, with WAAS active, it is 1.0 m. The co-ordinates of the regional AEM survey were set-up prior to the survey and the information was fed into the airborne navigation system.

2.5.5 GPS – Magnetic Gradiometer Loop

A NovAtel GPS antenna was installed on the front centre of the magnetic gradiometer loop to accurately record the position of the loop (Figure 5). GPS data were sampled every 0.2 seconds. The final GPS coordinates were differentially corrected by post-processing the gradiometer loop data along with GPS data obtained simultaneously from a base station setup nearby the survey area. Final horizontal coordinates are referenced to GDA94 MGA zone 54 and the height is referenced to the EGM96 geoid. The positional accuracy or circular error probability (CEP) is 1.0 m.

2.5.6 Inclinometer – Magnetic Gradiometer Loop

An Anlalog Devices ADIS16405 gyroscopic inclinometer was installed on the magnetic gradiometer loop (Figure 5) to accurately record the orientation of the loop with a sampling interval of 0.1 seconds.

The orientation of the magnetic gradiometer loop is determined by three rotation angles based on the local reference frame of the loop: roll (rotation about the x-axis), pitch (rotation about the y-axis) and yaw (rotation about the z-axis). The loop's reference frame is a right-handed coordinate system with the positive x-axis pointing in the flight direction, positive y-axis pointing to the left of the flight direction and the positive z-axis points vertically upward. Positive rotation for each angle is counter-clockwise about the axis when looking toward the origin.

2.5.7 Radar Altimeter

A Terra TRA 3000/TRI 40 radar altimeter was used to record terrain clearance. The antenna was mounted beneath the bubble of the helicopter cockpit (Figure 6) and is 2.5 metres below the GPS antenna located on the tail of the helicopter.

2.5.8 Laser Altimeter

A Schmitt Industries AR300 laser altimeter was used which has an altitude range 0.5 to 300m and accuracy ±5cm. The laser altimeter was located at the front of the horizontal magnetic gradient loop with a GPS antenna and inclinometer and the data was sampled at an interval of 0.2 seconds.

2.5.9 Digital Acquisition System

A Geotech data acquisition system recorded the digital survey data on an internal compact flash card. Data is displayed on an LCD screen as traces to allow the operator to monitor the integrity of the system. The data type and sampling interval as provided in Table 4.

Table 4: Acquisition sampling rates

Data Type	Sampling
TDEM	0.1 sec
Magnetometer	0.1 sec
GPS position	0.2 sec
Radar altimeter	0.2 sec
Laser altimeter	0.2 sec
Gyro Inclinometer	0.1 sec

2.6 Base Station

A combined magnetometer/GPS base station was utilized on this project. A Geometrics cesium vapour magnetometer was used as a magnetic sensor with a sensitivity of 0.001 nT. The base station recorded the magnetic field together with the GPS time at 1 Hz on a base station computer.

The base station magnetometer sensor was installed (30° 02.5125' S, 145° 56.8936' E), (30° 55.6216' S, 144° 24.9827' E), (032° 21.8527' S, 142° 24.4299' E); away from electric transmission lines and moving ferrous objects such as motor vehicles. The base station data were backed-up to the data processing computer at the end of each survey day.

2.7 Test Lines and Calibration Procedures

2.7.1 Full Waveform VTEM Calibration

The calibration is performed with the completely assembled VTEM system connected to the helicopter at the survey site on the ground. Measurements of the half-cycles are collected and used to calculate a sensor calibration consisting of a single stacked half-cycle waveform. The purpose of the stacking is to attenuate natural and man-made magnetic signals, leaving only the response to the calibration signal. The stacked half-cycle allows the transfer functions between the receiver and data acquisition system, $H_D(\omega)$, and current sensor and data acquisition system, $H_R(\omega)$, to be determined. These transfer functions are used as a part of the system response correction during processing to correct the half-cycle waveforms and data acquired on a survey flight to a common transfer function:

$$D(\omega) = [H_C(\omega)/H_D(\omega)]\ D_R(\omega)$$
$$A(\omega) = [H_C(\omega)/H_R(\omega)]\ A_R(\omega)$$

where $H_C(\omega)$ is the common transfer function, and $D_R(\omega)$ and $A_R(\omega)$ are the FFT's of the raw receiver and current sensor responses recorded by the data acquisition system.

This process allows for the receiver response, R(ω), to become independent of the sensor characteristics determined by the transfer functions $H_D(\omega)$ and $H_R(\omega)$ and acts similar to a deconvolution of the data.

$$R(\omega) = \frac{D(\omega)I(\omega)}{A(\omega)}$$

where, D(ω) is the FFT of the actual receiver data sample D(t), I(ω) is the FFT of a reference or "Ideal waveform" and A(ω) is the FFT of the actual waveform.

2.7.2 High Altitude Calibration

High altitude calibrations were conducted at the beginning, during, and end of each flight. The calibration's objective is to determine the EM "zero level" by climbing to an altitude of 1,000 metres above ground to measure the receiver's response absent of response due to the ground.

When at the required altitude, at least 60 seconds of data were acquired in normal operation mode. The final delivered dataset contains these processed windowed high altitude data for the twenty-three (23) survey flights in ASCII column format (Table 5).

Reference transmitter current and receiver voltage waveforms, each sampled at 192 kHz, were also recorded at high altitude for all survey flights. The recorded waveforms were transformed into an ideal form, having zero current at the beginning of the off-time, by the Full Waveform calibration (see Section 2.7.1). A graphical representation of a VTEM waveform is shown in Figure 5. The waveforms for each flight were also delivered in the final dataset in ASCII column format.

2.7.3 Plate Test

This test is performed on ground to verify the sensitivity of the system. An aluminium plate of known conductive response is positioned in alternated positions (vertical and horizontal) for about 10 seconds for three time measurements. Response of corresponding dB/dt and B-field data is then verified.

The Plate test was performed at the beginning of the survey. Result of the test performed on May 10th, 2014 is presented in a Geosoft database view in Appendix D.

2.7.4 Radar and Laser Altimeters

The purpose of radar and laser altimeter calibration is to verify the performance of the altimeter readings using the GPS height data as the reference.

The calibration was performed by flying over the same spot at various altitudes, ranging from 61m (200 ft) to 133m (435 ft) according to the radar altimeter which is positioned on the helicopter front. The selected spot in the Hungerford airport has known elevation and flat terrain (Figure 7). These tests were performed on March 27th, 2014.

Figure 7: Location of the radar and laser altimeter calibrations on Google Earth™ image

The calibration results are presented in Appendix D. The graphs of the GPS heights plotted against the radar and laser altimeter readings demonstrate that there is a linear relationship between all GPS and altimeter instruments (R^2 = 0.99), for the range of flying heights tested.

3. PERSONNEL

The following Geotech Ltd personnel were involved in the project.

<u>Field:</u>

Project Manager:	Leon Lovelock (Office)
Data QC:	Neil Fiset (Office)
Crew chief:	Kobus de Beer
Operator:	Jared White

The survey pilot and the mechanical engineer were employed directly by the helicopter operator – United Aero Helicopters

Pilot:	James Bolton-Riley
Mechanical Engineer:	n/a

<u>Office</u>:

Preliminary Data Processing:	Neil Fiset
Final Data Processing:	Timothy Eadie
Final Data QA/QC:	Geoffrey Plastow
Reporting/Mapping:	Liz Mathew

The data acquisition phase was carried out under the supervision of Andrei Bagrianski, P. Geo, Chief Operating Officer. The processing and interpretation phases were carried out under the supervision of Geoffrey Plastow, P. Geo, Data Processing Manager. The customer relations were looked after by Keith Fisk.

4. DATA PROCESSING AND PRESENTATION

Data compilation and processing were carried out using Geosoft OASIS Montaj software and software proprietary to Geotech Ltd.

4.1 Flight Path, Coordinates and Parallax Correction

The flight path data, recorded by the acquisition program as WGS 84 latitude/longitude, were differentially corrected using the base station GPS and converted into the GDA94 Datum, Map Grid of Australia Zone 54 coordinate system in Oasis Montaj.

Both sets of GPS coordinate, from helicopter GPS and magnetic gradiometer GPS, were linearly interpolated between each measurement sampled every 0.2 seconds to match the sampling rate of the TDEM and magnetic datasets at every 0.1 seconds.

The coordinates labelled "GradLoop_*" in Tables 7 and 8 refer to the position of the magnetic gradiometer GPS antenna located at the front of the magnetic gradiometer loop.

A further set of coordinates, labelled "EM_Mag_Data_*" were then calculated for the position halfway between the two magnetometers that are located on the left and right hand sides of the magnetic gradiometer loop. This position represents the centre of the magnetic gradiomter loop and is the point where the tow cable intersects the plane of the magnetic gradiometer loop. This was achieved by projecting backwards along the flight line by 6.25 m, the radius of the gradiometer loop, from the gradiometer loop GPS antenna position.

A parallax correction was applied to the EM data to account for the distance by which the EM transmitter-receiver loop lags behind the centre of the magnetic gradiometer loop. In this parallax correction the EM data are shuffled toward lower fiducial numbers by the nearest integer number of fiducials that it would take to travel the average horizontal distance Δx_2 (see Figure 8 and formulae below) which separates the centres of the magnetic gradiometer and EM loops based on the average helicopter speed for each line.

Thus the "EM_Mag_Data_*" coordinates are the set of coordinates that the EM and magnetic data are parallax corrected for, and to which all EM and magnetic data and interpretations should be referred.

4.2 Calculation of EM Transmitter-Receiver Loop Height

The EM transmitter-receiver loop height above ground was calculated from data from the radar altimeter located on the helicopter, and data from the laser altimeter and gyroscopic inclinometer located on the front of the magnetic gradiometer loop, and knowledge of the tow cable lengths.

The procedure requires calculation of the unknown vertical distance between the magnetic gradiometer loop and EM transmitter-receiver loop. This process is summarized in the formula below, where; laser is the laser altimeter measurement, radar is the radar altimeter measurement, l_1 is the length along the tow cable from the helicopter to the center of the gradiometer loop equal to 29.65 metres, l_2 is the length along the tow cable from the center of the gradiometer loop to the center of the transmitter-receiver loop equal to 12.35 meters, and δz is the vertical deflection of the front of the gradiometer loop from the center which can be calculated from the pitch angle and magnetic gradiometer loop radius of 6.25m. These variables are illustrated in Figure 8 showing the VTEM system with an exaggerated pitch.

$$\text{TxRx Height} = \text{laser} + \delta z - l_2 \left(\frac{\text{radar} - \text{laser} - \delta z}{l_1} \right)$$

$$\Delta x_2 = \sqrt{(l_2)^2 - (\Delta z_2)^2},$$

where,

$$\Delta z_2 = l_2 \left(\frac{\text{radar} - \text{laser} - \delta z}{l_1} \right).$$

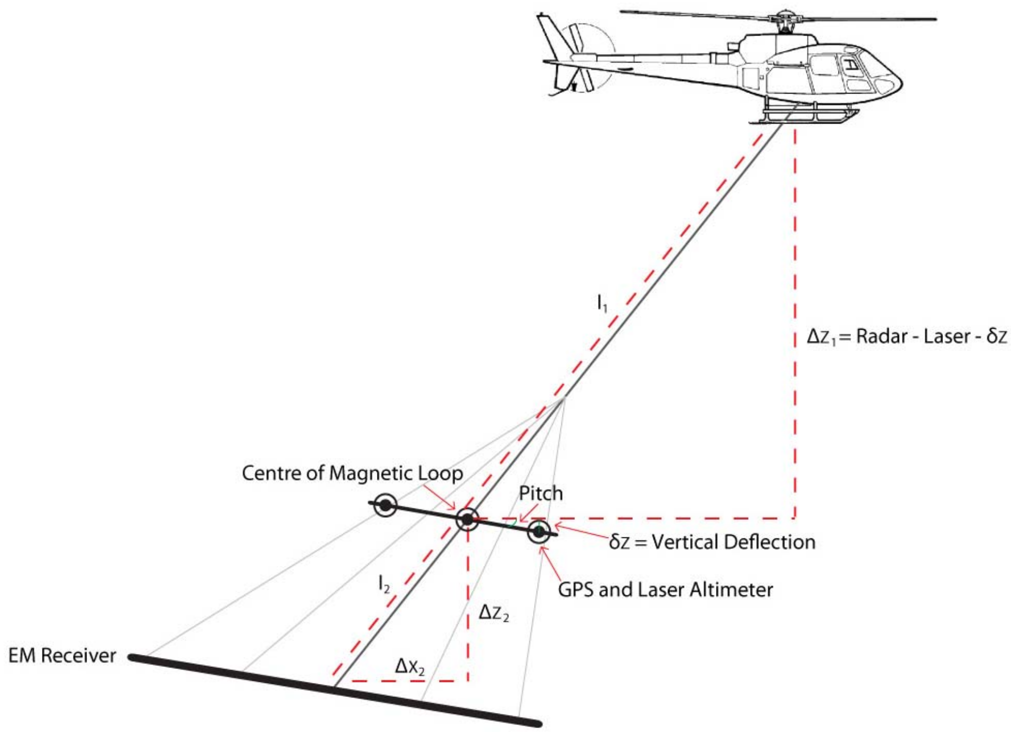

Figure 8: Calculation of EM transmitter loop height.

4.3 Digital elevation model

Two digital elevation models (DEMs) were calculated. They were calculated from the helicopter GPS and radar altimeter, and also from the magnetic gradiometer loop GPS and laser altimeter. The formulas used to calculate the DEMs are shown below.

$$\mathrm{DEM_{radar}} = (\mathrm{Z_{GPS\ Heli}} + \mathrm{N_{EGM96}} - \mathrm{N_{AUSGEOID09}}) - \mathrm{radar} - 2.5$$

$$\mathrm{DEM_{laser}} = (\mathrm{Z_{GPS\ GradLoop}} + \mathrm{N_{EGM96}} - \mathrm{N_{AUSGEOID09}}) - \mathrm{laser}$$

The term N_{EGM96} - $N_{AUSGEOID09}$, accounts for the difference between the EGM96 geoid, which the GPS heights are referenced to, and the AUSGEOID09, which both DEMs are referenced to. The 2.5 metre offset, for the radar altimeter derived DEM, accounts for the vertical separation between the helicopter GPS antenna located on the tail and the radar altimeter located below the noise of the helicopter.

On average the radar altimeter derived DEM is 4.5 metres higher than the laser altimeter derived DEM. The reason for this is unknown. However, the DEM_{radar} more closely matches the Shuttle Radar Topography Mission (SRTM) digital elevation model.

4.4 Electromagnetic Data

As the data are acquired by the data acquisition system on the helicopter, it goes through a digital filter to reject major sferic events and is stacked to further reduce system noise. Afterward, the streamed data is processed by applying a system response correction, B-field integration, time window binning, compensation, filtering, and leveling. Four stages of processing of the EM data have been delivered. They are denoted in the final point-located EM dataset (Table 5) as;

1. Raw (Raw),
2. Compensated (Comp),
3. Filtered (Flt),
4. Final (F).

The digital filtering process is a three stage filter used to reject major sferic events and reduce system noise. Local sferic activity can produce sharp, large amplitude events that cannot be removed by conventional filtering procedures. Smoothing or stacking will reduce their amplitude but leave a broader residual response that can be confused with geological phenomena. To avoid this possibility, a computer algorithm searches out and rejects the major sferic events. The data was then stacked using 15 half cycles, 0.3 seconds, to create a stacked half-cycle waveform at 0.1 second intervals. The stacking coefficients are tapered with a shape that approximates a Gaussian function.

During post-flight processing, the streamed data have a sensor response correction applied which corrects the receiver channels and current monitor to a common impulse response based on the Full Waveform calibration (see Section 2.7.1). The B-field data are calculated by integrating the dB/dt cycles from the 192 kHz streamed data. Then, the streamed data are converted into a set of time window channels (see Table 3) to reduce noise levels further. The output of this stage is the data denoted as “Raw” in Table 5.

The data have noise levels reduced further by the use of an EM compensation procedure which removes characteristic noise from each fiducial determined by the difference between the transmitter and bucking loop fields at the receiver during the flight. This is achieved by a statistical correlation between each time window channel and primary field measurement taken during the on-time. The data channels which have been processed to this point are denoted by “Compensated” in Table 5.

Next, filtering of the electromagnetic data was performed in two steps. The first is a 4 fiducial wide non-linear filter to eliminate any large spikes remaining in the dataset. The second filter is a low pass symmetric linear digital filter that has zero phase shift which prevents any lag or peak displacement from occurring, and it suppresses only variations with a wavelength less than about 1 second or 25 metres. The output of this stage is the data channels denoted as “Filtered” in Table 5.

To remove the remaining system response from the data, a “zero level” estimate was subtracted from the data at each fiducial. First, the “zero level” correction was applied which was calculated by linear interpolation of the high altitude backgrounds (see Section 2.7.2) recorded two or more times during each survey flight. Second, a statistical leveling correction was applied to the EM data which utilizes the high altitude data recorded for each flight and the survey line data to compute the additional leveling correction. This produces the EM data denoted as “Final” in Table 5.

VTEM has two receiver coil orientations. The axis of the Z-component coil is oriented parallel to the transmitter coil axis and both are nominally vertical. The axis of the X-component coil is oriented parallel to the ground and along the line-of-flight. This combined two-coil configuration provides information on the position, depth, dip and thickness of a conductor. Generalized modeling results of VTEM data, are shown in Appendix C.

In general X-component data produce cross-over type anomalies: from “+ to – “in the direction of flight for “thin” sub-vertical targets and from “- to +” in the direction of flight for “thick” targets. Z component data produce double peak type anomalies for “thin” sub vertical targets and single peak for “thick” targets.

The limits and change-over of “thin-thick” depends on dimensions of a TEM system (Appendix C, Figure C-16).

4.5 Conductivity Depth Imaging

A set of Conductivity Depth Images (CDI) were generated using EM Flow version 3.3, developed by Encom Technologies Pty Ltd. A total of forty-four (44) dB/dt Z component channels, starting from channel 5 (26 µsec) to channel 48 (10667 µsec), were used for the CDI calculation for the data collected with the regular pulse, and forty-five (45) dB/dt Z componenent channels ranging from channel 5 (26 µsec) to channel 49 (12250 µsec) were used for the short pulse . Time channel 4 (21 µsec) was not inputted to avoid artefacts caused by fitting this earliest channel which may have greater uncertainty. This time channel 4 can be affected by over or underestimation of the compensation. An averaged waveform at the receiver was used for the calculation since it was consistent for the majority of the flights with minor deviation from the average. The waveform used is consistent with those supplied and outlined in Table 8. The main steps to calculate the

CDI in EM Flow are described in the following points:

1. System definition (units, waveform shape and half period, system geometry and input data format)
2. Conversion from ASCII file format to Binary file format (smoothing option disabled)
3. Basis Function creation. Number of Taus equalled 40 (approximately equal to the number of channels). Tau range was 0.02 to 7.0 msec. Number of Eigenvectors was 12.
4. Deconvolution: PLS algorithm. Smoothing set to 0.2 and minimum length to 0. Normalization by absolute maximum. Error tolerance at 1.0e-04. No error weighting.
5. CDI Matrix Calculation: Tau range at all (1-40). Maximum altitude at 500 metres and maximum depth at 400 metres. Depth resolution of 1 metre. Depth of investigation cut-off factor equal to 1. Both exponential and layered models were generated.
6. Data export: Geosoft Line Database.

The final delivered CDI dataset (Table 7) contains estimated conductivities as an array with 80 elements with a depth resolution of 5 metres, for depths from 5 metres to 400 metres.

Conductivity Depth Slices were calculated from the 1 metre depth resolution data output from EM Flow by averaging conductivity values within the specified depth ranges, inclusively.

4.6 Horizontal Magnetic Gradiometer Data

The horizontal gradients data from the VTEM^{plus} are measured by two magnetometers 12.5 m apart on an independent magnetic gradiometer loop mounted 10m above the transmitter-receiver loop. A GPS and a gyro inclinometer help to determine the positions and orientations of the magnetometers. The data from the two magnetometers are corrected for position and orientation variations, as well as for the diurnal variations using the base station data.

The position of the centre of the horizontal magnetic gradiometer loop is calculated from the GPS utilizing an in-house processing tool in Geosoft. Following this total magnetic intensity is calculated at the center of the gradiometer loop by calculating the mean values from both sensors. In-line and cross-line gradient and advanced magnetic gradient products were not contracted for this project.

5. DELIVERABLES

5.1 Survey Report

This survey report describes the data acquisition, processing, and final presentation of the survey results. The survey report is provided in two paper copies and digitally in PDF format.

5.2 Digital Data

Point located data files in ASCII column format, with accompanying README header files that describe the data file content, were supplied for the processed EM and ancillary data. The delivered data channels listed in Table 5 for the regular survey lines and Table 6 for the short pulse survey lines. Refer to Table 3 for the time definitions for channels 4 to 49.

Table 5: Contents of the ASCII columns datasets for the regular pulse point located EM data

Channel name	Units	Description
GA_project		Geoscience Australia Project Number
GT_project		Geotech Ltd Project Number
Flight		Flight Number
Line		Line Number
Fiducial		Fiducial Number
Date		Date
Time	Seconds	Seconds since midnight local time
Bearing	Degrees	Flight Direction Azimuth
Heli_Longitude	Degrees	Helicopter GPS Longitude (GDA94)
Heli_Latitude	Degrees	Helicopter GPS Latitude (GDA94)
Heli_Easting	metres	Helicopter GPS Easting (GDA94, MGA54[†])
Heli_Northing	metres	Helicopter GPS Northing (GDA94, MGA54)
Heli_Height	metres	Helicopter GPS height above EGM96 Geoid
Heli_GPSTime	seconds	Helicopter GPS second of the GPS week
Radar_altimeter	metres	Helicopter radar altimeter height above ground
GradLoop_Longitude	degrees	Gradiometer Loop GPS Longitude (GDA94)
GradLoop_Latitude	degrees	Gradiometer Loop GPS Latitude (GDA94)
GradLoop_Easting	metres	Gradiometer Loop GPS Easting (GDA94, MGA54)
GradLoop_Northing	metres	Gradiometer Loop GPS Northing (GDA94, MGA54)
GradLoop_Height	metres	Gradiometer Loop GPS height above EGM96 Geoid
GradLoop_GPSTime	seconds	Gradiometer Loop GPS second of the GPS week
Laser_altimeter (Laser)	metres	Gradiometer Loop laser altimeter height above ground
Roll	degrees	Gradiometer Loop rotation about the in-line (x) axis
Pitch	degrees	Gradiometer Loop rotation about the cross-line (y) axis
Yaw	degrees	Gradiometer Loop rotation about the vertical (z) axis
EM_Mag_Data_Longitude	degrees	Derived longitude of centre of magnetic

Channel name	Units	Description
		gradiometer loop – reference point for EM and Magnetic data (GDA94)
EM_Mag_Data_Latitude	degrees	Derived latitude of centre of magnetic gradiometer loop – reference point for EM and Magnetic data (GDA94)
EM_Mag_Data_Easting	metres	Derived easting of centre of magnetic gradiometer loop – reference point for EM and Magnetic data (GDA94, MGA54)
EM_Mag_Data_Northing	metres	Derived northing of centre of magnetic gradiometer loop – reference point for EM and Magnetic data (GDA94, MGA54)
EM_Loop_Height	metres	Derived height of centre of the EM Loop above ground
Ground_elevation_laser	metres	Digital Elevation Model (Australian Height Datum) derived from laser altimeter and Gradiometer Loop GPS
Ground_elevation_radar	metres	Digital Elevation Model (Australian Height Datum) derived from radar altimeter and Helicopter GPS
Mag1L	nT	Measured Total Magnetic field - left sensor
Mag1R	nT	Measured Total Magnetic field - right sensor
Mag2L	nT	Diurnal and IGRF corrected Total Magnetic field - left sensor
Mag2R	nT	Diurnal and IGRF corrected Total Magnetic field - right sensor
Mag_average	nT	Total Magnetic field (average of left and right sensors)
Basemag	nT	Base station mag
IGRF_Tot	nT	IGRF Total Field
Tx_Current	Amps	Transmitter Current
Powerline_monitor		50 Hz power line monitor
SRawz[4-48]	pV/(A*m4)	Raw Z dB/dt data channels 4 to 48
SCompz[4-48]	pV/(A*m4)	Compensated Z dB/dt data channels 4 to 48
SFltz[4-48]	pV/(A*m4)	Filtered Z dB/dt data channels 4 to 48
SFz[4-48]	pV/(A*m4)	Final Z dB/dt data channels 4 to 48
BRawz[4-48]	(pV*ms)/(A*m4)	Raw Z B-Field data channels 4 to 48
BCompz[4-48]	(pV*ms)/(A*m4)	Compensated Z B-Field data channels 4 to 48
BFltz[4-48]	(pV*ms)/(A*m4)	Filtered Z B-Field data channels 4 to 48
BFz[4-48]	(pV*ms)/(A*m4)	Final Z B-Field data channels 4 to 48
SRawx[20-48]	pV/(A*m4)	Raw X dB/dt data channels 20 to 48
SCompx[20-48]	pV/(A*m4)	Compensated X dB/dt data channels 20 to 48
SFltx[20-48]	pV/(A*m4)	Filtered X dB/dt data channels 20 to 48
SFx[20-48]	pV/(A*m4)	Final X dB/dt data channels 20 to 48
BRawx[20-48]	(pV*ms)/(A*m4)	Raw X B-Field data channels 20 to 48
BCompx[20-48]	(pV*ms)/(A*m4)	Compensated X B-Field data channels 20 to 48
BFltx[20-48]	(pV*ms)/(A*m4)	Filtered X B-Field data channels 20 to 48
BFx[20-48]	(pV*ms)/(A*m4)	Final X B-Field data channels 20 to 48

†MGA54 = Map Grid of Australia Zone 54

Table 6: Contents of the ASCII columns datasets for the short pulse point located EM data

Channel name	Units	Description
GA_project		Geoscience Australia Project Number
GT_project		Geotech Ltd Project Number
Flight		Flight Number
Line		Line Number
Fiducial		Fiducial Number
Date		Date
Time	Seconds	Seconds since midnight local time
Bearing	Degrees	Flight Direction Azimuth
Heli_Longitude	Degrees	Helicopter GPS Longitude (GDA94)
Heli_Latitude	Degrees	Helicopter GPS Latitude (GDA94)
Heli_Easting	metres	Helicopter GPS Easting (GDA94, MGA54)
Heli_Northing	metres	Helicopter GPS Northing (GDA94, MGA54)
Heli_Height	metres	Helicopter GPS height above EGM96 Geoid
Heli_GPSTime	seconds	Helicopter GPS second of the GPS week
Radar_altimeter	metres	Helicopter radar altimeter height above ground
GradLoop_Longitude	degrees	Gradiometer Loop GPS Longitude (GDA94)
GradLoop_Latitude	degrees	Gradiometer Loop GPS Latitude (GDA94)
GradLoop_Easting	metres	Gradiometer Loop GPS Easting (GDA94, MGA54)
GradLoop_Northing	metres	Gradiometer Loop GPS Northing (GDA94, MGA54)
GradLoop_Height	metres	Gradiometer Loop GPS height above EGM96 Geoid
GradLoop_GPSTime	seconds	Gradiometer Loop GPS second of the GPS week
Laser_altimeter (Laser)	metres	Gradiometer Loop laser altimeter height above ground
Roll	degrees	Gradiometer Loop rotation about the in-line (x) axis
Pitch	degrees	Gradiometer Loop rotation about the cross-line (y) axis
Yaw	degrees	Gradiometer Loop rotation about the vertical (z) axis
EM_Mag_Data_Longitude	degrees	Derived longitude of centre of magnetic gradiometer loop – reference point for EM and Magnetic data (GDA94)
EM_Mag_Data_Latitude	degrees	Derived latitude of centre of magnetic gradiometer loop – reference point for EM and Magnetic data (GDA94)
EM_Mag_Data_Easting	metres	Derived easting of centre of magnetic gradiometer loop – reference point for EM and Magnetic data (GDA94, MGA54)
EM_Mag_Data_Northing	metres	Derived northing of centre of magnetic gradiometer loop – reference point for EM and Magnetic data (GDA94, MGA54)
EM_Loop_Height	metres	Derived height of centre of the EM Loop above ground
Ground_elevation_laser	metres	Digital Elevation Model (Australian Height Datum) derived from laser altimeter and Gradiometer Loop GPS
Ground_elevation_radar	metres	Digital Elevation Model (Australian Height Datum) derived from radar altimeter and Helicopter GPS

Channel name	Units	Description
Mag1L	nT	Measured Total Magnetic field - left sensor
Mag1R	nT	Measured Total Magnetic field - right sensor
Mag2L	nT	Diurnal and IGRF corrected Total Magnetic field - left sensor
Mag2R	nT	Diurnal and IGRF corrected Total Magnetic field - right sensor
Mag_average	nT	Total Magnetic field (average of left and right sensors)
Basemag	nT	Base station mag
IGRF_Tot	nT	IGRF Total Field
Tx_Current	Amps	Transmitter Current
Powerline_monitor		50 Hz power line monitor
SRawz[4-49]	pV/(A*m4)	Raw Z dB/dt data channels 4 to 49
SCompz[4-49]	pV/(A*m4)	Compensated Z dB/dt data channels 4 to 49
SFltz[4-49]	pV/(A*m4)	Filtered Z dB/dt data channels 4 to 49
SFz[4-49]	pV/(A*m4)	Final Z dB/dt data channels 4 to 49
BRawz[4-49]	(pV*ms)/(A*m4)	Raw Z B-Field data channels 4 to 49
BCompz[4-49]	(pV*ms)/(A*m4)	Compensated Z B-Field data channels 4 to 49
BFltz[4-49]	(pV*ms)/(A*m4)	Filtered Z B-Field data channels 4 to 49
BFz[4-49]	(pV*ms)/(A*m4)	Final Z B-Field data channels 4 to 49
SRawx[20-49]	pV/(A*m4)	Raw X dB/dt data channels 20 to 49
SCompx[20-49]	pV/(A*m4)	Compensated X dB/dt data channels 20 to 49
SFltx[20-49]	pV/(A*m4)	Filtered X dB/dt data channels 20 to 49
SFx[20-49]	pV/(A*m4)	Final X dB/dt data channels 20 to 49
BRawx[20-49]	(pV*ms)/(A*m4)	Raw X B-Field data channels 20 to 49
BCompx[20-49]	(pV*ms)/(A*m4)	Compensated X B-Field data channels 20 to 49
BFltx[20-49]	(pV*ms)/(A*m4)	Filtered X B-Field data channels 20 to 49
BFx[20-49]	(pV*ms)/(A*m4)	Final X B-Field data channels 20 to 49

Point located data files were supplied in ASCII column format, with accompanying README header files, for the processed conductivity depth imaging results and ancillary data. This included files for the regular survey lines and short pulse survey lines. The delivered data channels are listed in Table 7.

Table 7: Contents of the ASCII columns dataset for the point located CDI data

Channel name	Units	Description
GA_project		Geoscience Australia Project Number
GT_project		Geotech Ltd Project Number
Flight		Flight Number
Line		Line Number
Fiducial		Fiducial Number
Date		Date
Time	Seconds	Seconds since midnight local time
Bearing	Degrees	Flight Direction Azimuth
Heli_Longitude	Degrees	Helicopter GPS Longitude (GDA94)
Heli_Latitude	Degrees	Helicopter GPS Latitude (GDA94)
Heli_Easting	metres	Helicopter GPS Easting (GDA94, MGA54)
Heli_Northing	metres	Helicopter GPS Northing (GDA94, MGA54)
Heli_Height	metres	Helicopter GPS height above EGM96 Geoid
Heli_GPSTime	seconds	Helicopter GPS second of the GPS week
Radar_altimeter	metres	Helicopter radar altimeter height above ground

Channel name	Units	Description
GradLoop_Longitude	degrees	Gradiometer Loop GPS Longitude (GDA94)
GradLoop_Latitude	degrees	Gradiometer Loop GPS Latitude (GDA94)
GradLoop_Easting	metres	Gradiometer Loop GPS Easting (GDA94, MGA54)
GradLoop_Northing	metres	Gradiometer Loop GPS Northing (GDA94, MGA54)
GradLoop_Height	metres	Gradiometer Loop GPS height above EGM96 Geoid
GradLoop_GPSTime	seconds	Gradiometer Loop GPS second of the GPS week
Laser_altimeter	metres	Gradiometer Loop laser altimeter height above ground
Roll	degrees	Gradiometer Loop rotation about the in-line (x) axis
Pitch	degrees	Gradiometer Loop rotation about the cross-line (y) axis
Yaw	degrees	Gradiometer Loop rotation about the vertical (z) axis
EM_Mag_Data_Longitude	degrees	Derived longitude of centre of magnetic gradiometer loop – reference point for EM and Magnetic data (GDA94)
EM_Mag_Data_Latitude	degrees	Derived latitude of centre of magnetic gradiometer loop – reference point for EM and Magnetic data (GDA94)
EM_Mag_Data_Easting	metres	Derived easting of centre of magnetic gradiometer loop – reference point for EM and Magnetic data (GDA94, MGA54)
EM_Mag_Data_Northing	metres	Derived northing of centre of magnetic gradiometer loop – reference point for EM and Magnetic data (GDA94, MGA54)
EM_Loop_Height	metres	Derived height of centre of the EM Loop above ground
Ground_elevation_laser	metres	Digital Elevation Model (Australian Height Datum) derived from laser altimeter and Gradiometer Loop GPS
Ground_elevation_radar	metres	Digital Elevation Model (Australian Height Datum) derived from radar altimeter and Helicopter GPS
Mag1L	nT	Measured Total Magnetic field - left sensor
Mag1R	nT	Measured Total Magnetic field - right sensor
Mag2L	nT	Diurnal and IGRF corrected Total Magnetic field - left sensor
Mag2R	nT	Diurnal and IGRF corrected Total Magnetic field - right sensor
Mag_average	nT	Total Magnetic field (average of left and right sensors)
Basemag	nT	Base station mag
IGRF_Tot	nT	IGRF Total Field
Tx_Current	Amps	Transmitter Current
Powerline_monitor		50 Hz power line monitor
Conductivity[0-79]	S/m	Conductivity Depth Imaging from 5 to 400 metres depth for every 5 metres
Cond_Depth_Slice_0_5m	S/m	Conductivity Depth Slice between 0 and 5

Channel name	Units	Description
		metres depth
Cond_Depth_Slice_5_10m	S/m	Conductivity Depth Slice between 5 and 10 metres depth
Cond_Depth_Slice_10_15m	S/m	Conductivity Depth Slice between 10 and 15 metres depth
Cond_Depth_Slice_15_20m	S/m	Conductivity Depth Slice between 15 and 20 metres depth
Cond_Depth_Slice_20_30m	S/m	Conductivity Depth Slice between 20 and 30 metres depth
Cond_Depth_Slice_30_40m	S/m	Conductivity Depth Slice between 30 and 40 metres depth
Cond_Depth_Slice_40_60m	S/m	Conductivity Depth Slice between 40 and 60 metres depth
Cond_Depth_Slice_60_100m	S/m	Conductivity Depth Slice between 60 and 100 metres depth
Cond_Depth_Slice_100_150m	S/m	Conductivity Depth Slice between 100 and 150 metres depth
Cond_Depth_Slice_150_200m	S/m	Conductivity Depth Slice between 150 and 200 metres depth
Cond_Depth_Slice_200_300m	S/m	Conductivity Depth Slice between 200 and 300 metres depth
Cond_Depth_Slice_300_400m	S/m	Conductivity Depth Slice between 300 and 400 metres depth

Data files were supplied in ASCII column format, with accompanying README header files, for the 192 kHz sampling of the waveform acquired at high altitude for every flight. The delivered waveform data are listed in Table 8.

Table 8: Contents of the ASCII columns datasets for the waveform data

Channel name	Units	Description
Flight		Flight number
Time	Seconds	Time of current sample
Tx_Current	Amps	Transmitter Current
Rx_Voltage	volts	Receiver voltage

Respectfully submitted[2],

Neil Fiset
Geotech Ltd

Timothy Eadie
Geotech Ltd

Geoffrey Plastow, P. Geo.
Data Processing Manager
Geotech Ltd

October, 2014

[2] Final data processing of the EM and magnetic data were carried out by Timothy Eadie, from the office of Geotech Ltd in Aurora, Ontario, under the supervision of Geoffrey Plastow, P.Geo. Data Processing Manager.

APPENDIX A

SURVEY BLOCK LOCATION MAP

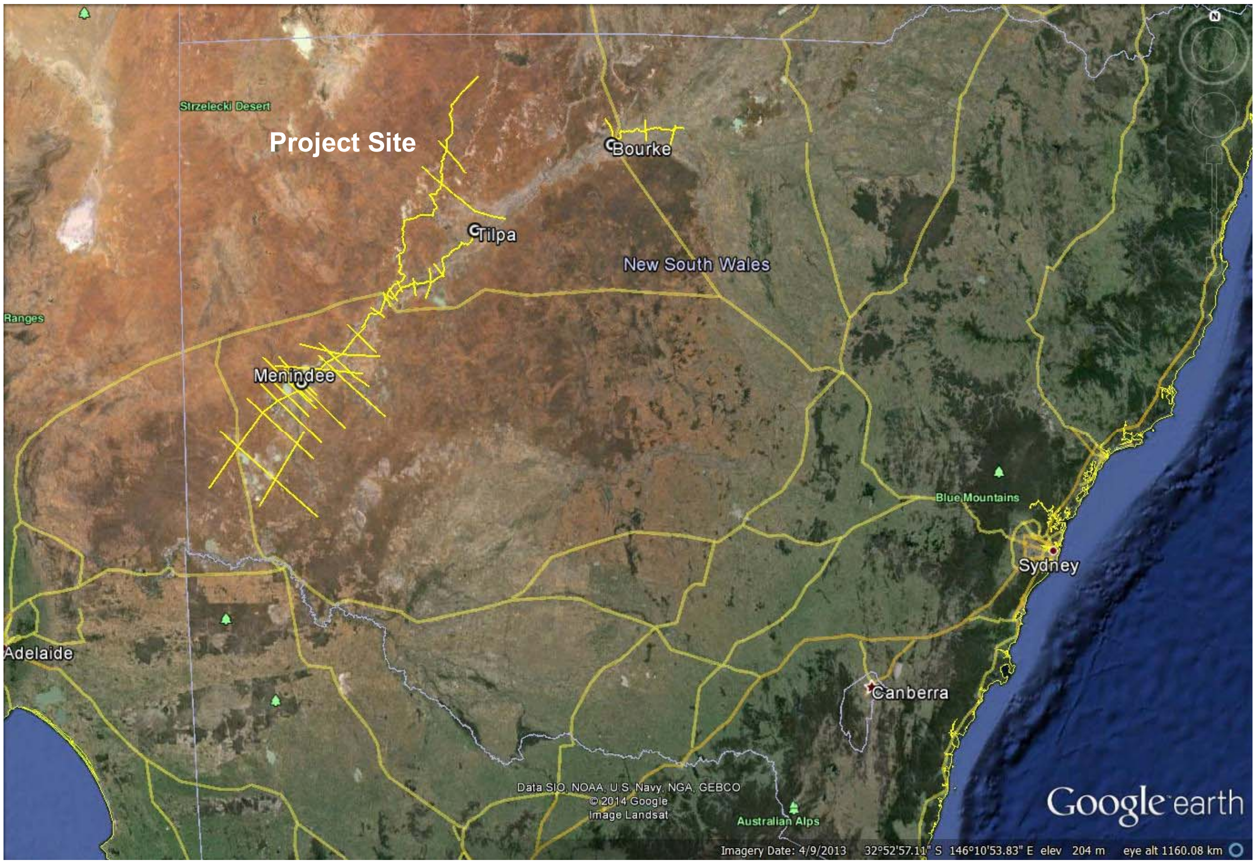

Overview of the Survey Area

APPENDIX B

Flight Line Summary

Line number	Start Fiducial	End Fiducial
100	84678	99284
101	9835	35067
200	56310	70524
300	72065	80506
400	66862	108032
500	18184	54672
600	66365	84070
601	66022	76045
700	13650	46622
800	19412	58116
900	10315	30774
901	21149	49024
1000	62438	87889
1100	32035	74099
1200	85809	106765
1300	12017	29761
1400	44897	52136
1401	16147	41964
1402	104100	119427
1403	19286	71314
1500	99145	110228
1501	12894	43177
1502	50261	70497
1600	10282	28657
1601	35182	57558
1700	21250	29525
1800	15256	52503
1801	10233	31332
1900	61192	69039
2000	48302	56047
2100	66457	74536
2200	92563	99963
2201	11957	13114
2202	15037	31218
2203	39033	59042
2300	73839	86714
2400	45102	50585
2500	77204	89144

Line number	Start Fiducial	End Fiducial
2600	94035	103707
2700	15967	33349
2800	74170	115805
2801	42726	45085
2802	47246	74332
2803	15022	40179
2804	73496	109738
2805	33277	42605
2901	16273	35189
2902	41934	69413
3000	49479	62143
3100	10150	29515
3200	54307	61980
3201	61733	74666

Short Pulse

Line number	Start Fiducial	End Fiducial
505	78400	92062
506	10174	31249
605	26134	54561

APPENDIX C

GENERALIZED MODELING RESULTS OF THE VTEM SYSTEM

Introduction

The VTEM system is based on a concentric or central loop design, whereby, the receiver is positioned at the centre of a transmitter loop that produces a primary field. The wave form is a bi-polar, modified square wave with a turn-on and turn-off at each end.

During turn-on and turn-off, a time varying field is produced (dB/dt) and an electro-motive force (emf) is created as a finite impulse response. A current ring around the transmitter loop moves outward and downward as time progresses. When conductive rocks and mineralization are encountered, a secondary field is created by mutual induction and measured by the receiver at the centre of the transmitter loop.

Efficient modeling of the results can be carried out on regularly shaped geometries, thus yielding close approximations to the parameters of the measured targets. The following is a description of a series of common models made for the purpose of promoting a general understanding of the measured results.

A set of models has been produced for the Geotech VTEM® system dB/dT Z and X components (see models C1 to C15). The Maxwell TM modeling program (EMIT Technology Pty Ltd Midland, WA, AU) used to generate the following responses assumes a resistive half-space. The reader is encouraged to review these models, so as to get a general understanding of the responses as they apply to survey results. While these models do not begin to cover all possibilities, they give a general perspective on the simple and most commonly encountered anomalies.

As the plate dips and departs from the vertical position, the peaks become asymmetrical.

As the dip increases, the aspect ratio (Min/Max) decreases and this aspect ratio can be used as an empirical guide to dip angles from near 90º to about 30º. The method is not sensitive enough where dips are less than about 30º.

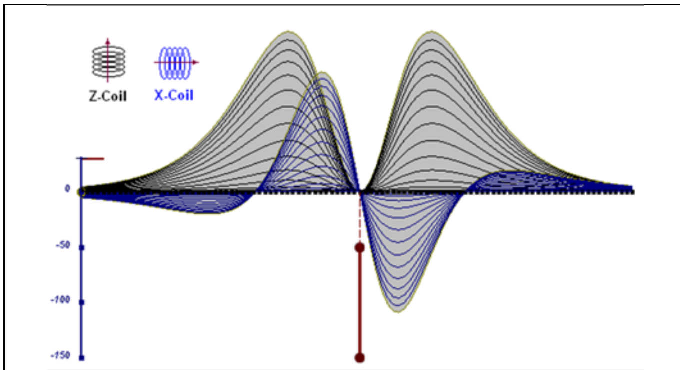

Figure C-1 vertical thin plate

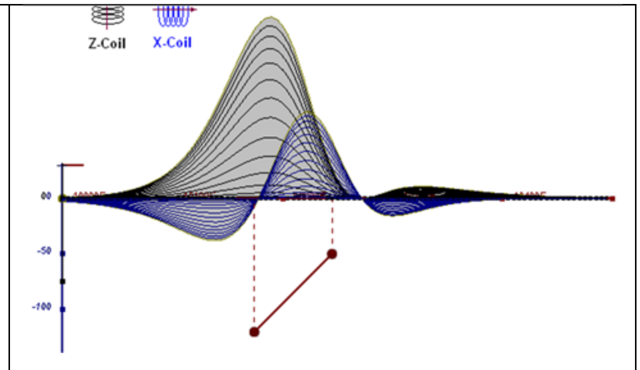

Figure C-2: inclined thin plate

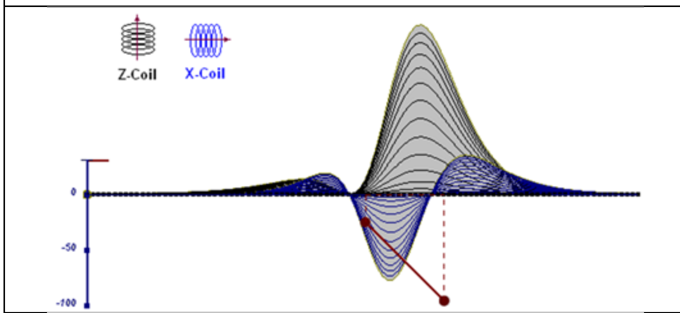

Figure C-3: inclined thin plate

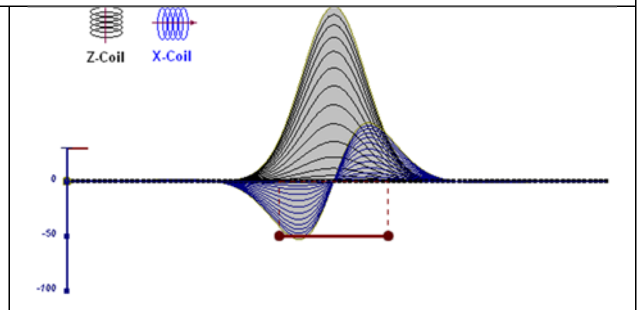

Figure C-4: horizontal thin plate

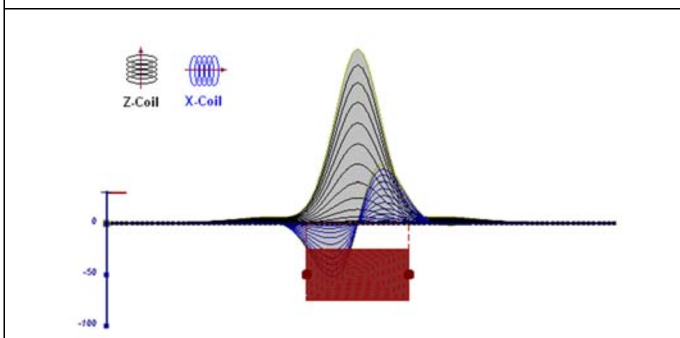

Figure C-5: horizontal thick plate (linear scale of the response)

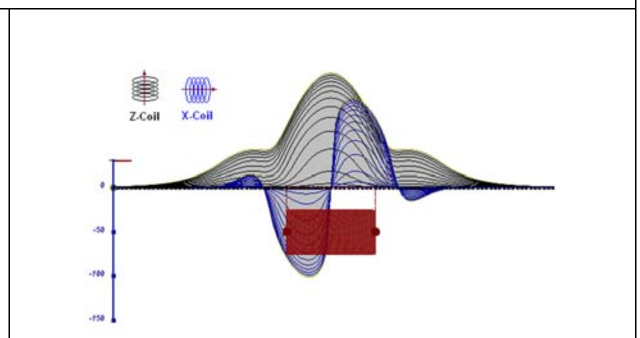

Figure C-6: horizontal thick plate (log scale of the response)

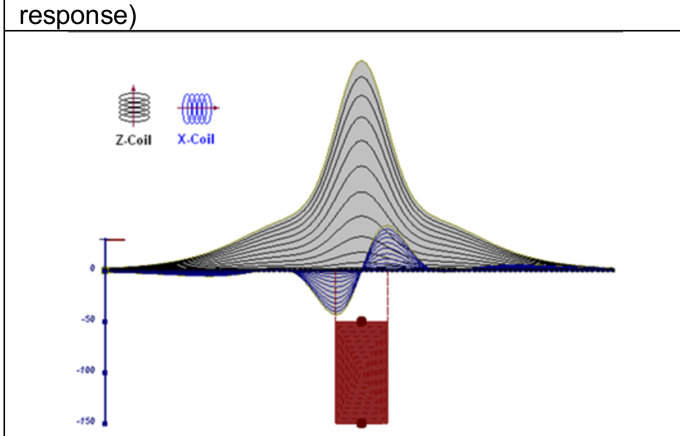

Figure C-7: vertical thick plate (linear scale of the response). 50 m depth

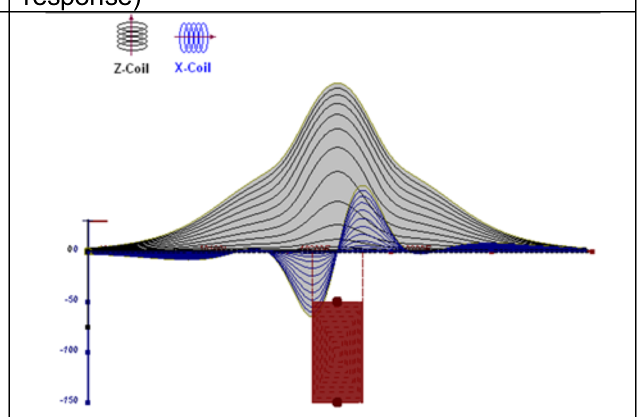

Figure C-8: vertical thick plate (log scale of the response). 50 m depth

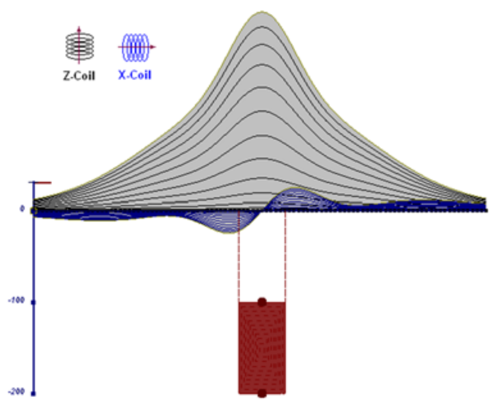

Figure C-9: vertical thick plate (linear scale of the response). 100 m depth

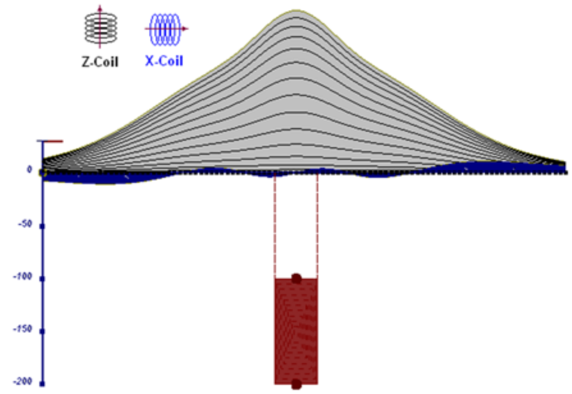

Figure C-10: vertical thick plate (linear scale of the response). Depth/hor.thickness=2.5

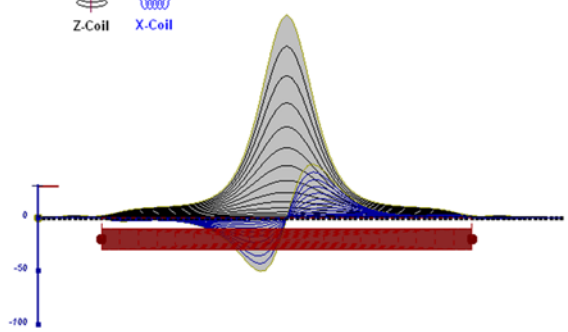

Figure C-10: horizontal thick plate (linear scale of the response)

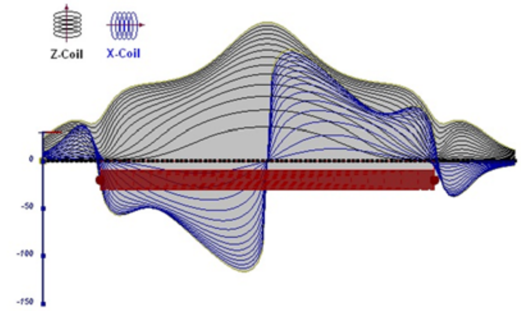

Figure C-11: horizontal thick plate (log scale of the response)

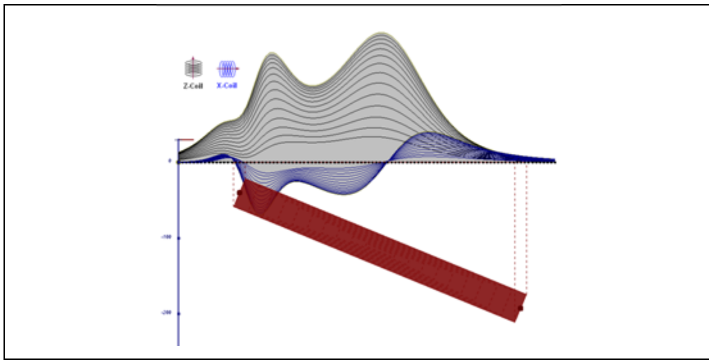

Figure C-12: inclined long thick plate

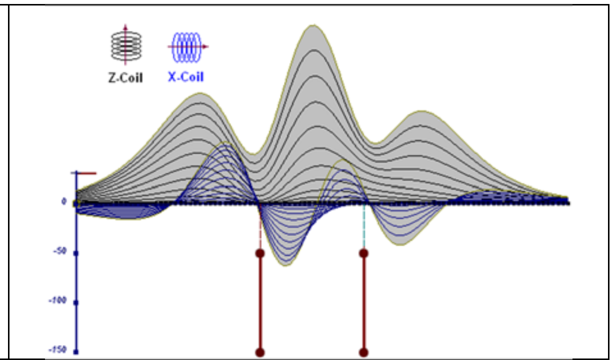

Figure C-13: two vertical thin plates

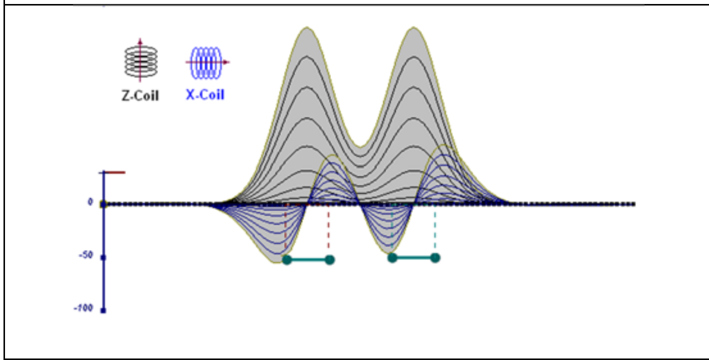

Figure C-14: two horizontal thin plates

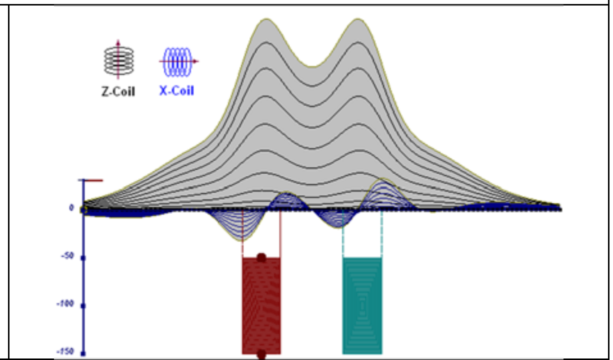

Figure C-15: two vertical thick plates

The same type of target but with different thickness, for example, creates different form of the response:

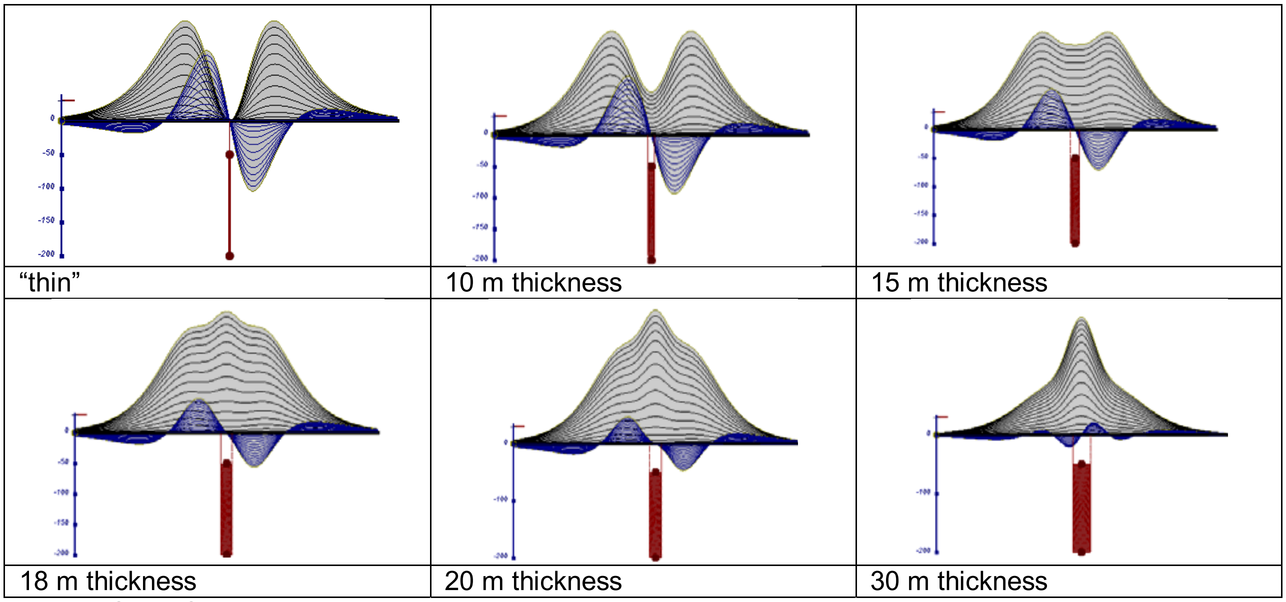

Figure C-16: Conductive vertical plate, depth 50 m, strike length 200 m, depth extends 150 m.

Alexander Prikhodko, PhD, P.Geo
Geotech Ltd.

September 2010

APPENDIX D

TEST SITES AND CALIBRATIONS

PLATE / ALUMINUM TEST

When the aluminum plate is horizontal with respect to the loop, measured signal will show positive response, indicating a proper polarity (see H1 in figure below).

Figure below present the plate/aluminum test results performed on May 10th, 2014.

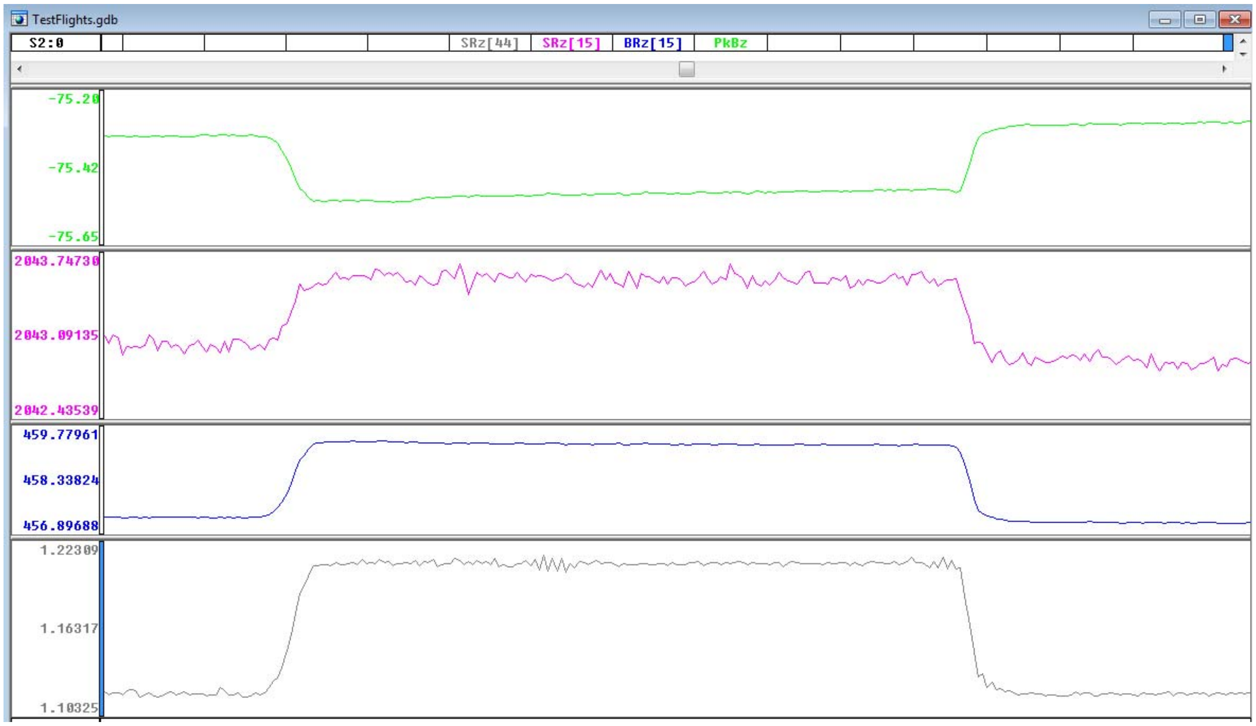

RADAR AND LASER ALTIMETER CALIBRATION TESTS

Test Date: March 27, 2014 Hungerford Airport
Ground Elevation at test site is 144 metres.

Database Line	**Helicopter GPS Height** (m)	**Radar Altimeter** (m)	**Magnetic Gradiometer GPS Height** (m)	**Laser Altimeter** (m)
10060	208	61	182	40.6
10075	222	76	196	56.6
10090	240	93	215	73.7
10115	261	116	236	95.5
10130	279	133	255	114.3